Molecular Crystals and Liquid Crystals Science and Technology. Section A. Molecular Crystals and Liquid Crystals

Publication details, including instructions for authors and subscription information:
http://www.tandfonline.com/loi/gmcl19

Spin Crossover, Liesst, and Niesst-Fascinating Electronic Games in Iron Complexes

Philipp Gütlich [a]

[a] Institut für Anorganische Chemie und Analytische Chemie, Johannes Gutenberg-Universität, D-55099, Mainz, Germany

Version of record first published: 04 Oct 2006

To cite this article: Philipp Gütlich (1997): Spin Crossover, Liesst, and Niesst-Fascinating Electronic Games in Iron Complexes, Molecular Crystals and Liquid Crystals Science and Technology. Section A. Molecular Crystals and Liquid Crystals, 305:1, 17-40

To link to this article: http://dx.doi.org/10.1080/10587259708045044

Mol. Cryst. Liq. Cryst., 1997, Vol. 305, pp. 17–40
Reprints available directly from the publisher
Photocopying permitted by license only

SPIN CROSSOVER, LIESST, AND NIESST - FASCINATING ELECTRONIC GAMES IN IRON COMPLEXES

PHILIPP GÜTLICH
Institut für Anorganische Chemie und Analytische Chemie,
Johannes Gutenberg-Universität, D-55099 Mainz, Germany

Abstract: Coordination compounds of transition metal ions with open-shell electron configurations may exhibit dynamic electronic structure phenomena depending on the nature of the coordinating ligand sphere. The change of spin state with temperature („thermal spin crossover") and light-induced electron transfer processes leading to long-lived metastable states are among the most fascinating electronic games encountered in transition metal compounds and are presently under intensive study by chemists and physicists.The first part of this lecture will survey briefly some highlights of previous work and present recent results on thermal spin crossover in iron(II) compounds. The second part of the lecture will focus on selected examples of „Light-Induced Excited Spin State Trapping" (LIESST), with special emphasis on the occurrence of bistability and cooperative interactions during LIESST relaxation. The last part of the lecture will be devoted to „Nuclear Decay-Induced Excited Spin State Trapping"(NIESST), the unique experiment which allows one to make use of the nuclear disintegration of ^{57}Co $\rightarrow$ ^{57}Fe as an „internal light source" to generate such photophysical aftereffects as aliovalent charge and anomalous spin states, and to detect and characterize such metastable states simultaneously by time-integral and time-differential Mössbauer emission spectroscopy. Results from lifetime measurements by Mössbauer as well as optical techniques prove that the same relaxation mechanism applies to both phenomena, LIESST and NIESST.

INTRODUCTION

Beside the various magnetic properties there are numerous dynamic electronic structure phenomena in transition metal compounds, particularly of the 3d series, which have attracted much attention in recent years for both the sake of fundamental research as well as for eventual application in electronic devices. Mixed valency,[1,2] valence tautomerism[3,4] with spontaneous spin transition in a metal center,[5,6] changes of spin state induced by heat, pressure, light, and nuclear decay,[7] and light-induced electron transfer leading to long-lived metastable states[8,9,10,11] are some of the fascinating electronic games, to name a few. All have in common that the compound under study exhibits a change of electronic ground state upon application of a certain external perturbation leading to a new state differing in the electronic and/or molecular structure. Figure 1 shows a schematic drawing of two potential wells with the vibronic energies of a molecule in two different states, 1 and 2, differing in their valence, spin, conformational, or structural state, as a function of

the nuclear coordinate along a one-dimensional vibrational mode (for simplicity). Coexistence between the two states can be reached, if the energy difference between the lowest vibronic levels of each state is on the order of, or comparable to, the thermal energy: $\Delta E = E_2^0 - E_1^0 \approx k_B T$ (k_B is the Boltzmann constant).

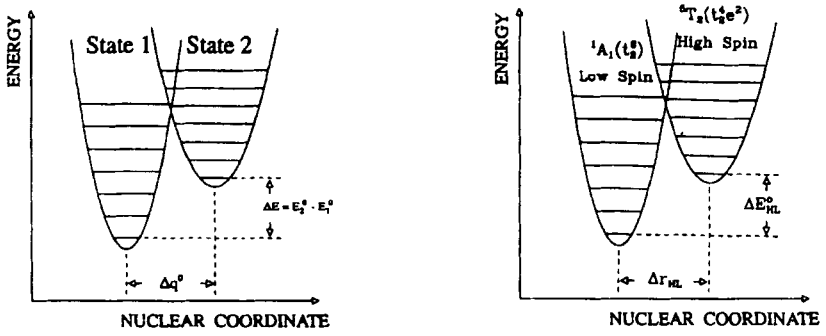

FIGURE 1 Vibronic energy (schematic) of a one-dimensional vibrational mode of a molecule fluctuating between two states 1 and 2 differing in their electronic and/or molecular structure. The condition for coexistence of the two states (bistability) is $\Delta E = E_2^0 - E_1^0 \approx k_B T$ (E_1, E_2 are the lowest vibronic energy levels and r_1, r_2 the corresponding equilibrium normal coordinates).

FIGURE 2 Schematic representation of the potential wells for the LS($^1A_1$) and the HS($^5T_2$) states of an iron(II) spin crossover complex. The nuclear coordinate is the metal-ligand bond length r(Fe-L). Thermal spin crossover occurs if $\Delta E_{HL}^0 \approx k_B T$.

The chemical equilibrium between the two states is strongly temperature dependent. Whether one actually observes the two states as static phases with a certain spectroscopic tool depends on the fluctuation rates k_{12} and k_{21}. These, of course, depend upon the energy barrier between the two states. Only if the reciprocal of the rates k_{12} and k_{21} are longer than the characteristic „time window" of the spectroscopic method used for detection can one „see" the two states as static phases with their characteristic sharp-line spectra. In this case one may speak of a *bistable system*. The molar fractions of the interconverting molecules (states) change with temperature or, at a given temperature, with pressure. This change may be gradual (continuous) or abrupt, or may even occur with a hysteresis (discontinuous). These properties may be used in applications of such bistable compounds as temperature or pressure sensors and in thermal and optical switching devices.[12,13]

One particular class of bistable compounds which has enjoyed much attention by many research groups are coordination compounds undergoing thermal spin transition (spin crossover), a process which is well established to occur in complexes of 3d metal ions with d^4 up to d^7 electron configuration.[14,15] In this case, state 1 in Figure 1 refers to the low spin (LS) state, and state 2 to the high spin (HS) state. This phenomenon has been known for more than sixty years. Cambi and his coworkers first reported, in the early thirties, on temperature-dependent changes of spin state in iron(III) tris-dithiolate complexes.[16] More than thirty years later, Baker and Bobonich[17] reported the first iron(II) spin crossover compound, the nowadays called classical $[Fe(phen)_2(NCS)_2]$ system (phen = 1,10-phenanthroline). Many additional compounds followed and launched a very active

field of research on spin crossover in transition metal compounds. Many cobalt(II) compounds (d^7),[18] a couple of cobalt(III) complexes(d^6),[19,20] some manganese(III) compounds (d^4),[21] and even chromium(II) (d^4) compounds[22] are also known to undergo thermal spin transition. Octahedral iron(II) spin crossover compounds exhibiting low spin (LS) $\leftrightarrow$ high spin (HS) transition, in the framework of ligand field theory termed as $^1A_1(t_{2g}^6) \leftrightarrow {}^5T_2(t_{2g}^4e_g^2)$ in the approximation of O_h symmetry, have been investigated extensively using a variety of physical techniques such as magnetic susceptibility measurements, optical, vibrational, and Mössbauer spectroscopy, heat capacity and diffraction methods, magnetic resonance, EXAFS, and positron anihilation. Many review articles have appeared in the literature,[7,23-28] covering all kinds of chemical, physical, and mechanical influences on the spin transition behaviour, thermodynamics and kinetics, and a variety of theoretical approaches have been developed to describe the cooperative spin transition in crystalline spin crossover systems.

In the course of our studies of thermal spin transition in crystalline iron(II) compounds we have discovered that interconversion between the LS and HS states can also be induced by irradiation with light of the appropriate wave length into characteristic absorption bands, whereby the newly generated metastable state may have practically infinitely long lifetimes, at least at sufficiently low temperatures.[29,30] This effect of „Light-Induced Excited Spin State Trapping" (LIESST) appears to be common to iron(II) compounds exhibiting thermal spin crossover and looks promising for future applications in optical devices. The mechanism of LIESST has been elucidated[31] and the dynamics of all intersystem crossing processes involved has been explored quantitatively.[32]

Earlier work in our laboratory on the physical and chemical aftereffects of the nuclear decay, by electron capture (EC), of radioactive ^{57}Co embedded in cobalt(II) or iron(II) coordination compounds has led to the observation of metastable HS states of iron(II) in Mössbauer emission spectra,[33,34] even in complexes with strong ligand fields where LS-iron(II) is the thermodynamically stable state. Later on, through the discovery of the LIESST phenomenon, it has turned out that the nature of these metastable HS states, generated via nuclear disintegration as a, so to speak, internal light source, which we now denote as „Nuclear Decay-Induced-Excited Spin State Trapping" (NIESST), are the same as those generated by LIESST. In fact, results from lifetime measurements using fast optical techniques after LIESST and time-differential Mössbauer emission measurements after NIESST lend support to the conclusion that both phenomena possess the same relaxation mechanism.

It is the purpose of this lecture, to present recent results from ongoing research on spin crossover, LIESST, and NIESST in iron(II) complexes. For a summary of earlier work the reader is referred to the review articles mentioned above.[7,28]

THERMAL SPIN CROSSOVER

The condition for thermal spin crossover to occur in iron(II) complexes is schematically illustrated by the two-potential-well picture of Figure 2.

There may be, as a rough estimate, some 150 to 200 iron(II) compounds known to undergo thermal spin transition. Most of them occur in the solid state, although some are also known to occur in liquid solution. A short review of the synthetic strategies in preparing spin crossover compounds has recently been given in ref. 28. The ligand field strength can be altered (fine-tuned) by ligand replacement or by introducing a more or less bulky substituent in the ligand molecule causing steric hindrance and in this way in-

fluencing the metal-ligand bond distance, which influences the ligand field strength.[14,15] This way it is possible in a rather controlled manner to come close to the critical field strength where the condition for thermal spin crossover to take place is met (see Figure 2), or to move towards weaker or stronger ligand fields, i.e. the stability regions of HS or LS compounds. One has also learned that substituting iron isotypically by, for instance, zinc, or by replacement of the non-coordinating anion or solvent molecules in the crystal lattice can influence the spin transition behaviour, i.e. the spin transition curve $\gamma_{HS}(T)$, dramatically. This may be considered unambiguous evidence for the existence of cooperative interactions (see below). These are responsible for the ocurrence of various types of spin transition curves: gradual, abrupt, stepwise, or with hysteresis.[7] Thermal spin transition in liquid solution, where interactions between the spin state changing molecules can be neglected, always reflect gradual $\gamma_{HS}(T)$ curves which can be reproduced by a simple Boltzmann distribution over all vibronic levels of the HS and LS states. Gradual $\gamma_{HS}(T)$ curves, however, are also encountered in solid spin crossover systems if the cooperative interactions become negligibly weak.

It was recognized already in the early stage of spin crossover studies from heat capacity measurements[35] that this phenomenon is almost entirely entropy driven, with an effective entropy gain of ca. 50 to 80 $Jmole^{-1}K^{-1}$ [7,24,27] on going from the LS to the HS state. Only approximately one quarter of this gain arises from the change in spin multiplicity, $\Delta S = S_{HS} - S_{LS} = R[\ln(2S+1)_{HS} - \ln(2S+1)_{LS}]$. The main contribution comes from the much higher (intra- and intermolecular) vibrational degrees of freedom in the HS state as compared to the LS state (cf. the higher vibrational density in the HS potential well of Figure 2). The effective enthalpy change $\Delta H = H_{HS} - H_{LS}$ is typically on the order of 10 to 20 $kJ\,mole^{-1}$ on going from the LS to the HS state.[7,24,27]

Mechanism of Spin Crossover in Solids

A successful model for the quantitative interpretation of spin transition in solids should explain all the different types of measured $\gamma_{HS}(T)$ curves. The HS fraction $\gamma_{HS}(T)$, as derived from Mössbauer spectra (in the slow relaxation limit) or from optical spectra, is the natural order parameter of the spin transition. Various attempts to describe quantitatively the different types of spin transition curves $\gamma_{HS}(T)$ (gradual, abrupt, hysteresis, step) have been communicated in the literature.[7,23,27] In fact, they mostly reproduce successfully the measured $\gamma_{HS}(T)$ curves, but lack more or less the connection to the actual mechanism, i.e. the processes in the lattice that are responsible for the spin state changes in the metal centers in a cooperative fashion. A brief survey of such spin crossover models has been given in references 7,23,27. Another model, which is based on elasticity theory and, in fact, correlates the shape of the measured $\gamma_{HS}(T)$ curves with the strength of long-range elastic interactions and allows one to express the interaction parameters in terms of observable quantities like elastic (bulk) modulus and Poisson ratio σ, has been developed by H. Spiering in our group.[36-39]

Long-Range Elastic Interactions

The most important experimental finding for the interpretation of the interaction mechanism in spin crossover solids is the drastic metal-donor atom bond-length change accompanying the spin transition,[25,40] this bond length being some 10 % longer in the HS state than in the LS state.The resulting impact on the lattice can be viewed as an anisotropic deformation process through long-range elastic interactions. The elasticity theory explains the infinite extent of such interactions as a result of the *image pressure* on the boundary

of finite crystals.[41] Consider, for instance, the LS→HS transition with increasing temperature in a finite mixed crystal containing LS, HS, and M complex molecules (M = Zn, Co, etc.) as sketched on the right-hand side of Figure 3. The entropy-driven conversion from LS to HS increases not only the volume of the complex molecule drastically (because of the transfer of two electrons from the weakly bonding t_{2g} orbitals to the antibonding e_g^* orbitals, cf. Figure 2), but may also change the shape of the molecules. Both effects have been illustrated in Figure 3. The close proximity of such noncubic dilatation centers (*point defects*) gives rise to dipole-dipole interaction (*direct interaction*). This is the possible explanation for the preferred formation of pairs of complexes of like spin (HS-HS, LS-LS) or unlike spin (HS-LS) on a short-range correlation scale (*short-range interactions*), which, to our present knowledge, are believed to be responsible for the steps observed in the transition curves of some spin crossover systems (see below). The coupled phonon system of the lattice „carries the message" of the formation of point defects due to spin state conversion through the lattice up to the surface of the crystal. The condition of a stress-free surface of the finite crossover lattice leads to an *image interaction* between the elastic defects. For illustration of the image interaction mechanism one may consider the simple case of spherical dilatation centers[41] as sketched on the left of Figure 3. The LS→HS conversion of an ensemble of such defects (on raising the temperature) causes the crystal to expand. The volume change ΔV^{∞} of the crystal is directly related to the volume change due to each center (indicated by the dark shaded section in Figure 3). In the case of a finite crystal, the stress-free boundary condition leads to a dilatation of the crystal which is larger than ΔV^{∞} by the so-called image volume change ΔV^{im} (indicated by the unshaded outer section); thus the total volume change (for a stress-free crystal after the spin state conversion) is $\Delta V = \Delta V^{\infty} + \Delta V^{im} = \gamma_0 \Delta V^{\infty}$. The *Eshelby constant* $\gamma_0 = 3(1-\sigma)/(1+\sigma)$ with $1 \leq \gamma_0 \leq 3$ relates the overall volume change ΔV of the finite crystal to the dilatational defect ΔV^{∞}. The effect of the surface may thus be viewed as the impact of a negative pressure from the outside,[42] which decreases the pressure inside the crystal and thus leads to facilitated formation of further HS centers. Conversely, an initial HS→LS transition (with decreasing temperature) is accompanied by an additional compression due to the surface causing further HS→LS transitions in a cooperative manner.

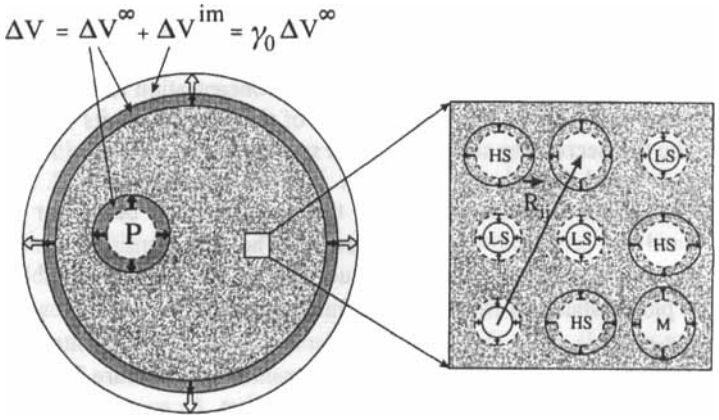

FIGURE 3 Schematic illustration of the elastic interaction in spin crossover solids. Left: dipole-surface (image) interaction. Right: dipole-dipole (direct) interaction.

The macroscopic lattice deformation accompanying a spin transition in solids is reflected by the observable deformation tensor including both the change of the volume and the shape of the unit cell.[43,44] These deformations are related by Hooke's law to stresses via the elastic properties of the crystal lattice and thus contribute to the Gibbs free energies of the crystal as elastic energies. The phenomenological thermodynamic treatment follows the *solid solution theory* of Slichter and Drickamer,[45] and the cooperative interaction energy is parameterized in the Bragg-Williams approximation.[27,39] To test this model of elastic interactions we have investigated the influence of metal dilution on the shape of the spin transition curve in mixed crystals with variable iron concentration x.[36,46,47] The Gibbs free energy per complex molecule, g_x, in a mixed crystal system of HS, LS, and M complexes (M = Zn, Co, etc.) is

$$g_x = x[\gamma_{HS}\, g_{HS} + (1 - \gamma_{HS})g_{LS} - Ts_{mix}(\gamma_{HS})] + (1 - x)g_{Zn} + x\, g_{int}(\gamma_{HS},x,T) + g_{lat}. \qquad (1)$$

g_{HS} and g_{LS} are the Gibbs free energies of the HS and LS states, g_{Zn} that of the host lattice, and g_{lat} refers to the Gibbs free energy of the residual lattice, taken as independent of γ_{HS}. $g_{int}(\gamma_{HS},x,T)$ is the interaction energy per Fe complex molecule. The mixing entropy is $s_{mix}(\gamma_{HS}) = - k_B[\gamma_{HS} \ln\gamma_{HS} + (1-\gamma_{HS})\ln(1-\gamma_{HS})]$; contributions to the mixing entropy independent of γ_{HS} have been omitted. As the interaction energy per complex molecule must vanish at infinite dilution , $g_{int}(\gamma_{HS},x\rightarrow 0,T) \rightarrow 0$, the equilibrium condition $\delta g_x/\delta\gamma_{HS} = 0$ yields the Boltzmann type population (with partition function Z) according to

$$\gamma_{HS}(T) = Z_{HS}(T)/[Z_{HS}(T) + Z_{LS}(T)]. \qquad (2)$$

From the expansion of the Gibbs free energy and ordering the terms up to second order in γ_{HS}, a contribution of interaction energies

$$g_{int}(\gamma_{HS},x,T) = \gamma_{HS}\ \Delta - \gamma_{HS}^2 \cdot \Gamma \qquad (3)$$

is obtained, where the coefficients Δ and Γ are the phenomenological interaction constants (in the Bragg-Williams approximation). These quantities are related to the bulk modulus, Eshelby constant (or Poisson ratio), and the molecular volumes of the HS, LS, and M constitutent molecules.[7,36] They are on the order of $\Delta(x) \approx 300$ cm^{-1} and $\Gamma(x) \approx 150$ cm^{-1} and decrease steadily with decreasing iron concentration to zero at $x \rightarrow 0$.

A comprehensive summary of the basic features of the model and its successful application to describe the decreasing steepness of the spin transition curves with decreasing iron concentration in metal-diluted mixed crystals is given in references 7,28. So far we have investigated the effect of metal dilution on the spin transition behaviour in the picolylamine[36,47,48] and the propyltetrazole complexes.[49] The spin transition curves $\gamma_{HS}(T)$ derived from the area fractions of the Mössbauer spectra recorded at variable temperature in case of the pic-crystals and from the area fractions of the $^1A_1 \rightarrow {}^1T_1$ absorption band in case of the ptz-crystals show the same dependence on the iron concentration: the $\gamma_{HS}(T)$ curves become more and more gradual and the transition temperature $T_{½}$ ($\gamma_{HS} = 0.5$) shifts to lower temperatures with decreasing iron concentration. As an example, Figure 5 shows the transition curves $\gamma_{HS}(x,T)$ from optical absorption measurements on single crystals of $[Fe_xZn_{1-x}(ptz)_6](BF_4)_2$; the temperature dependent absorption spectra for a single crystal with x = 0.87 are depicted in Figure 4.

Short-Range Interactions

The Bragg-Williams approach has proven to be a very good approximation for the interpretation of the long-range interactions, since for the spherical part of the elastic interaction in an isotropic medium, there is no direct short-range interaction that could give rise to correlations between HS and LS molecules. The image pressure is ubiquitous and effectively extends to infinity. The occurrence of step-like spin transitions, however, which was first seen in case of $[Fe(2\text{-pic})_3]Cl_2 \cdot EtOH$ [51] and later found to occur in other spin crossover compounds[52,53] lends support to the conclusion that short-range correlations appear to be active in this case and are, in fact, supposed to be the cause of such steps. Strong support for this conclusion comes from heat capacity measurements on the picolylamine complex.[54,55] Jakobi et al. have derived the mixing entropy as a function of temperature from the measured C_p data and compared it with calculations of the mixing entropy under the assumption of random distribution of HS and LS molecules. Whereas the calculated temperature function of S_{mix}(random) shows a maximum in the step region of $\gamma_{HS}(T)$, the experimental data of S_{mix}(exp) are significantly reduced. This reduction of entropy has been interpreted in terms of an ordering of HS and LS molecules.

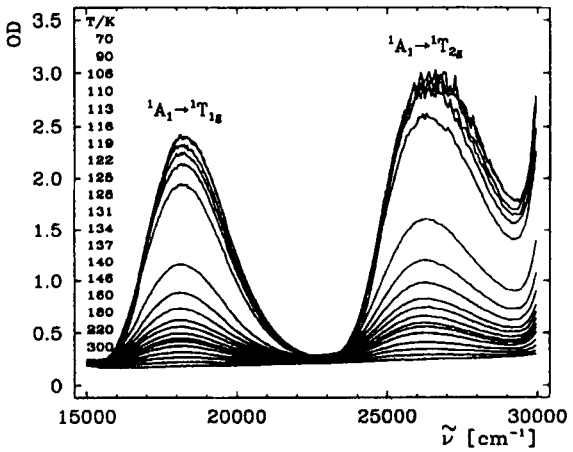

FIGURE 4 Temperature dependence of the optical density OD of the $^1A_1 \rightarrow {}^1T_1$ and the $^1A_1 \rightarrow {}^1T_2$ absorption bands of $[Fe_{0.87}Zn_{0.13}(ptz)_6](BF_4)_2$ (from ref. 50).

In a recent theoretical study, Kohlhaas et al.[56] have applied the Monte Carlo method to reproduce the two-step spin transition as well as the gradual lowering of $T_{1/2}$ with increasing x in the $[Fe_xZn_{1-x}(2\text{-pic})_3]Cl_2 \cdot EtOH$ mixed crystals. Both long-range interactions (predominantly accounting for the effect of metal dilution) and short-range interactions of antiferromagnetic type (HS-LS) with nearest neighbors and of ferromagnetic type (HS-HS, LS-LS) with next nearest neighbors (accounting for the occurrence of the step) in a simple cubic lattice have been included in the treatment. The results are shown in Figure 6. The simulation reproduces well the occurrence of the step in the transition curve of the pure spin crossover crystal (x = 1) and its disappearence upon dilution with zinc. The agreement between the simulated and measured transition curves is very good.

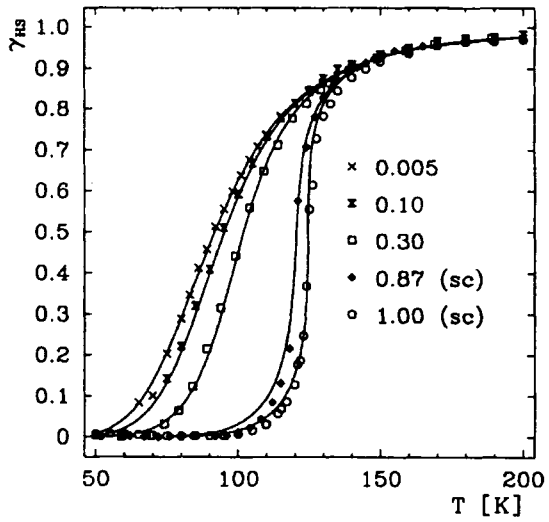

FIGURE 5 Transition curves $\gamma_{HS}(x,T)$ from optical absorption measurements $[Fe_xZn_{1-x}(ptz)_6](BF_4)_2$ in the high temperature structure R3i. In the cases of x = 0.87 and 1.0 the structure was preserved by supercooling (sc) (from ref. 49).

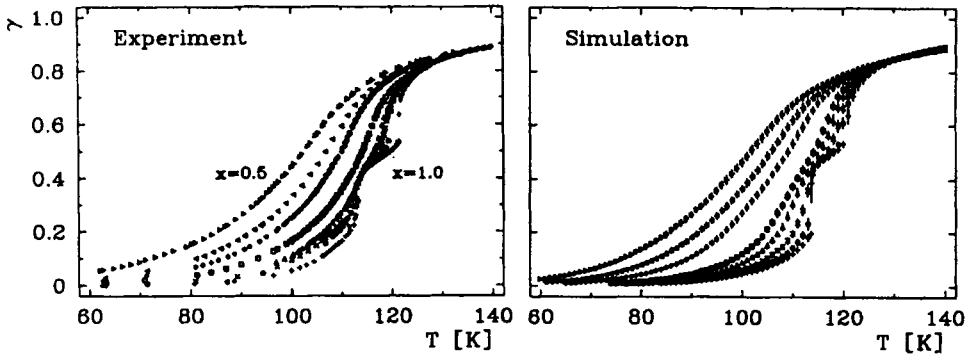

FIGURE 6 The effect of metal dilution in $[Fe_xZn_{1-x}(2\text{-pic})_3]Cl_2 \cdot EtOH$. Comparison of experimental data[39] (x = 1.00, 0.98, 0.94, 0.89, 0.86, 0.70, 0.60, 0.50) and Monte Carlo simulations. The transition temperatures decrease with decreasing x.

The same Monte Carlo method with similar assumptions has been used successfully to describe the influence of pressure on the shape of the spin transition curve of $[Fe(2\text{-pic})_3]Cl_2 \cdot EtOH$.[56] As can be seen from Figure 7, the step disappears under pressure, and the transition curves are shifted to higher temperatures with increasing pressure. The agreement between simulation and experiment is again excellent. This influence of pressure on the spin transition behaviour is, of course, conceivable in view of the known *drastic* shortening of the metal-ligand bond length accompanying the HS→LS conversion. Pressure studies have also been carried out with other spin crossover systems with dif-

ferent transition temperatures $T_{1/2}$,[57-60] with the same result of stabilizing the LS state under pressure. It is clear that such material may be used, after appropriate calibration, to design pressure sensors.

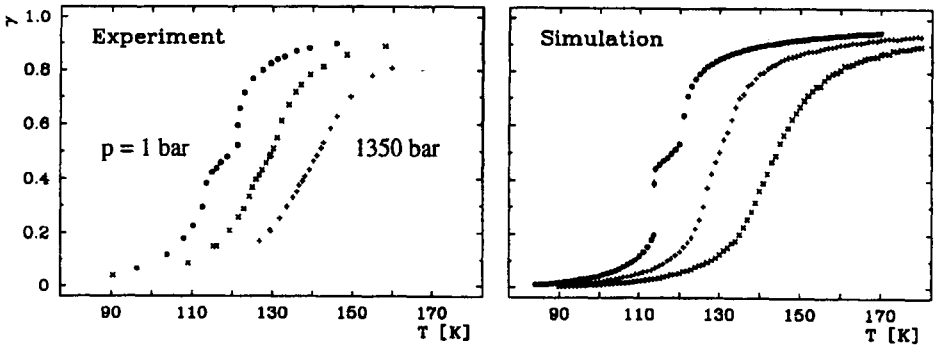

FIGURE 7 The effect of pressure on the spin transition curves of $[Fe(2pic)_3]Cl_2 \cdot EtOH$. Comparison of experimental data (p = 1, 600, 1350 bar)[39] and Monte Carlo simulations. The transition temperatures increase and the step in the transition curve disappears with increasing pressure.

The occurrence of steps in spin transition curves has been a particular focus of various research groups lately, both from the experimental and theoretical point of view. Real et al.[53] have simulated the two-step transition in the binuclear complex $[Fe(bt)(NCS)_2]_2(bpym)$ (bt = 2,2'-bi-2-thiazoline, bpym = 2,2'-bipyrimidine) assuming a random mixture of entities of four combinations of states, LS-LS, LS-HS, HS-LS, HS-HS, where the energies of the degenerate LS-HS and HS-LS pairs are equal and somewhat lower than the mean of the energies of LS-LS and HS-HS pairs, thus favouring HS-LS formations. This treatment is along the lines of Sasaki and Kambara,[61,62] who have introduced a cooperative Jahn-Teller coupling of the 3d electrons to the molecular deformation. Restricting themselves to the special case of a two-sublattice structure with HS-LS stabilization between, and HS-LS destabilization within, the sublattices, they succeeded with the first simulation of a two-step spin transition[63] within the mean field approximation. This has also been the starting point of Bousseksou et al.[64] in their attempt to simulate the two-step transition in $[Fe(2\text{-}pic)_3]Cl_2 \cdot EtOH$. It must be pointed out, however, that the validity of the assumption of a two-sublattice-structure in this case is questionable, since there is no evidence for it from X-ray data.[43] A more accurate treatment of the interaction leading to steps has been obtained by approaches beyond the molecular field approximation. Takahashi,[65] Bolvin and Kahn,[66] and Linares et al.[67] have used the Monte Carlo method for the study of hysteresis assuming destabilizing HS-LS „antiferromagnetic" interactions. Linares et al.[68] have also applied the Monte Carlo technique to model the two-step transition in the binuclear complex $[Fe(bt)(NCS)_2]_2(bpym)$ considering both intra and inter dimer interactions. In contrast to the above discussed Monte Carlo treatment of Kohlhaas et al.,[36] these models[53, 61-68] all neglect infinite range interactions which arise from the change of volume and shape of the complexes upon spin state conversion.

Changes of Crystal Structure Accompanying a Spin Transition

Crystal structure determination of spin crossover compounds, both above and below the transition temperature $T_{1/2}$, has been a most important part of spin crossover research ever since scientists started trying to explore the details of „why" and „how" spin transition in solids take place. The crystal structures of a number of spin crossover compounds and their changes as a consequence of spin state transition have been well characterized and discussed in many reports.[25] One has learned that the spin transition may occur without a crystallographic phase change (with the same space group above and below $T_{1/2}$). The $[Fe(2\text{-pic})_3]Cl_2 \cdot EtOH$ complex is a representative of this class.[40,43] It is worth mentioning in this context that the bromide analog, $[Fe(2\text{-pic})_3]Br_2 \cdot EtOH$, shows a hysteris in the spin transition curve, but no crystallographic phase change.[43] In numerous cases, however, the spin transition is accompanied by a first order crystallographic phase transition indicated by a hysteresis in the $\gamma_{HS}(T)$ curve. The $[Fe(ptz)_6](BF_4)_2$ compound is a member of this group. Here the often posed question arises as to whether the crystallographic phase transition triggers the spin transition or vice versa. We could answer this question in case of the $[Fe(ptz)_6](BF_4)_2$ complex in a recent experiment.[49] We rapidly first cooled down a single crystal of $[Fe(ptz)_6](BF_4)_2$ such that the high temperature R3i phase was preserved (no crystallographic phase transition took place). On raising the temperature we observed the spin transition as shown by the filled circles in Figure 8. On cooling down and warming up slowly, the spin transition is accompanied by a crystallographic phase change and shows hysteresis (see Figure 8). It is clear that in this case the spin transition triggers the crystallographic phase transition.

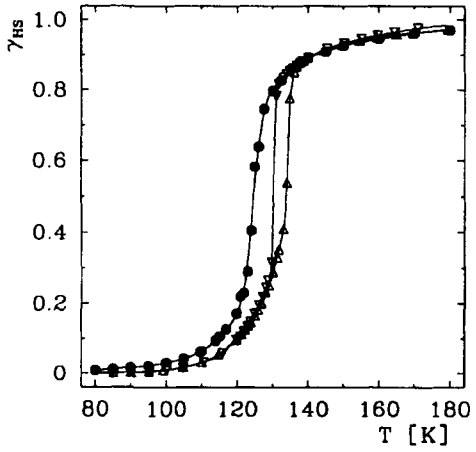

FIGURE 8 Thermal spin transition in $[Fe(ptz)_6](BF_4)_2$: (o) in the supercooled R3i phase, (∇,Δ) accompanied by the strucutral phase transition R3i↔P1i on slowly cooling and warming (from references 7,49).

It was also found from powder X-ray measurements on $[Fe_xZn_{1-x}(ptz)_6](BF_4)_2$ that the crystallographic phase transition disappears for $x < 0.44$; below this concentration the lattice deformation is found to be directly related to the spin transition.[49] The lattice deformation tensor (including the changes of volume and shape) derived from these measurements[49] together with the elasticity constants determined by Brillouin spectroscopy in a separate study[69] have enabled us to calculate the interaction constant. We found the calculated value to be ca. 20 % lower than the experimental value derived from the

metal dilution studies (Δ/cm^{-1} = 258 (theory), 318 (exp.); Γ/cm^{-1} = 135 (theory), 169 (exp.) at 125 K). This rather good agreement suggests the validity of our model of elastic interaction, i.e. the cooperativity in crystalline spin crossover compounds appears to be of an elastic nature. $[Fe(ptz)_6](BF_4)_2$ is the only spin crossover complex so far, for which the complete set of seven elasticity constants was measured directly.[69]

LIGHT-INDUCED EXCITED SPIN STATE TRAPPING (LIESST)

$[Fe(ptz)_6](BF_4)_2$

In 1984 we found, in the course of our studies on iron(II) compounds exhibiting thermal spin crossover, that switching between the HS and LS states can also be achieved by irradiation with light of different wave lengths.[29,30] The LS($^1A_1$) state is converted to the HS($^5T_2$) state by irradiating with green light (using the 514 nm wavelength of an Ar ion laser or a Xe arc lamp with filters) into the $^1A_1 \rightarrow {}^1T_1$ absorption band. The metastable

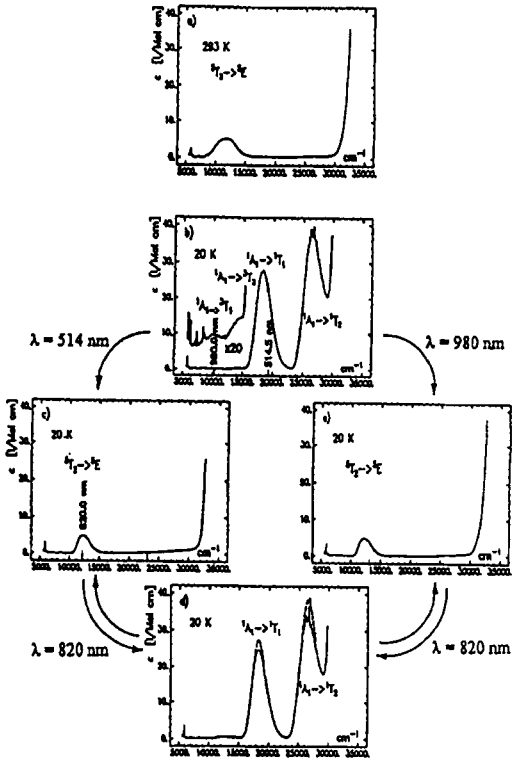

FIGURE 9 Single crystal UV/VIS absorption spectra along the crystallographic c-axis of the R3i (high temperature) phase of $[Fe(ptz)_6](BF_4)_2$ showing the d-d transitions (a) at 293 K, (b) at 20 K (after rapidly cooling), (c) after irradiation at 514.5 nm (at 20 K), after subsequent irradiation at 820 nm (at 20 K) (d) or at 980 nm (at 20 K) (e). The enlarged inset (x20) in (b) shows the weak singlet-triplet transitions. All spectra show the molar absorption coefficient ε[l/(mole·cm)] versus the wave number 1/λ [1/cm] (from ref. 31).

HS($^5T_2$) state may have practically infinitely long lifetimes at sufficiently low temperatures. The phenomenon has been termed „Light-Induced Excited Spin State Trapping (LIESST)". Soon after this discovery on the $[Fe(ptz)_6](BF_4)_2$ complex, Hauser[70] demonstrated that the reverse process, the conversion of the metastable HS($^5T_2$) state can be converted by irradiating the crystal with red light (using the 820 nm wavelength of a Krypton laser or a Xe lamp with filters) into the $^5T_2 \rightarrow {}^5E$ absorption band („Reverse-LIESST"). These light-induced conversions are demonstrated by the single crystal absorption spectra of Figure 9.

The originally proposed mechanism[29,30] was later fully elucidated;[31] it is explained with the Jablonski diagram of Figure 10. Excitation with green light (514.5 nm) affords the $^1A_1 \rightarrow {}^1T_1$ transition followed by two intersystem crossing processes $^1T_1 \rightarrow {}^3T_1 \rightarrow {}^5T_2$. The metastable state is trapped in the potential well of the HS($^5T_2$) state, which is well separated by Δr_{HL}, the difference in the metal-ligand bond distances between the HS and the LS states, from the potential well of the LS($^1A_1$) state. Hauser showed[31] that the light-induced conversion from the LS($^1A_1$) to the HS($^5T_2$) state can also be achieved by directly irradiating into the weak $^1A_1 \rightarrow {}^3T_1$ absorption band using light in the near infrared (980 nm from a Ti sapphire laser), as proved by the step from (b) to (e) in Figure 9.

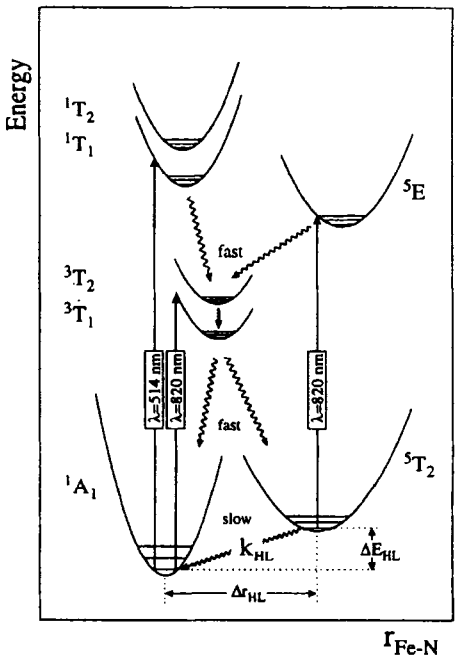

FIGURE 10 Schematic illustration of the mechanism of LIESST and reverse-LIESST of a d^6 complex in the spin crossover range. The d-d transitions to the excited ligand field states are denoted by arrows (with the experimental values of $[Fe(ptz)_6](BF_4)_2$) and the radiationless relaxation processes by wavy lines (from 7).

Radiative back relaxation to the LS state is formally forbidden and can only occur radiationless by warming the crystal and releasing the trapped energy into the lattice. This was nicely demonstrated in a calorimetric measurement on single crystal of $[Fe(ptz)_6](BF_4)_2$ using a custom-built microcalorimeter;[71] the results are shown in Figure 11.[72] The crystal was rapidly cooled down to ca. 20 K and converted by green light from the LS to the HS state. The crystal was then slowly warmed up. The energy P[mW] needed to raise the temperature was recorded as a function of T[K]. The peak pointing downwards reflects the release of energy which is trapped in the metastable LIESST state. As can be seen from the figure, this energy release begins at ca. 50 K and is finished near 85 K. The dotted (triangular) data refer to the experiment without light-induced spin state conversion. As the temperature reaches the region near 130 K, a strong upward peak begins to show up. This peak reflects the energy needed for the thermal LS→HS conversion together with the accompanying crystallographic phase transition.

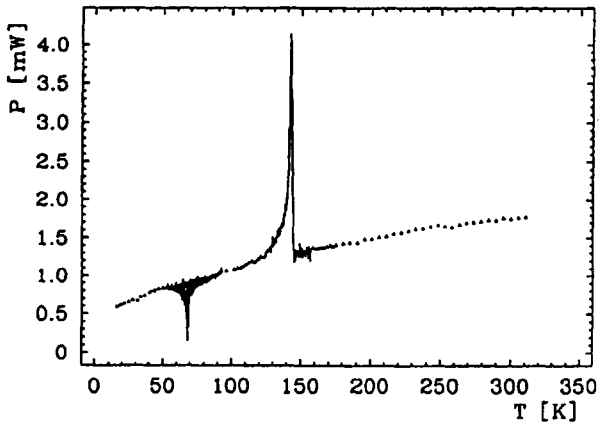

FIGURE 11 Calorimetric (DSC) measurement of the latent heat trapped in the metastable LIESST state (the energy release is indicated by the downward peak with a minimum near 70 K) and of the energy needed to induce the thermal spin transition together with the accompanying crystallographic phase transition (upward peak with a maximum near 135 K) in a single crystal of $[Fe(ptz)_6](BF_4)_2$.[72]

The reverse-LIESST process (see Figure 10) uses red light (ca. 820 nm) to excite the metastable $^5T_2$ state to the ^5E state, which subsequently decays radiationless, again involving two intersystem crossing processes, via $^5E \rightarrow {}^3T_1 \rightarrow {}^1A_1$ back to the LS($^1A_1$) state. LIESST and reverse-LIESST are favored by spin-orbit coupling and are therefore fast switching processes (nanoseconds or faster). Hauser[7,32] has carefully studied the dynamics of LIESST and reverse-LIESST and described quantitatively the relaxation of the LIESST states on the basis of a non-adiabatic multiphonon theory originally proposed by Jortner et al.[73] The two most important quantities in this relaxation model, which determine the lifetime of the LIESST state, are the energy difference ΔE_{HL}^0 between the lowest vibronic levels of the HS and the LS states on the one hand and the change of the metal-donor atom (ligand) bond length Δr_{HL} on the other hand, i.e. the relative vertical and horizontal displacements of the HS and LS potential wells. The smaller ΔE_{HL}^0 (*reduced energy gap law)* and the larger Δr_{HL}, the longer is the lifetime of the LIESST state. The relaxation kinetics was also studied by Mössbauer spectroscopy, either by conveniently

recording subsequent spectra of the decaying LIESST state (on a 10 minute time scale) or by line-shape analysis of Mössbauer relaxation spectra (on a 100 ns time scale) in connection with Blume's relaxation theory.[74,75]

$[Fe(mtz)_6](BF_4)_2$

Replacing the propyl substituent by a methyl group in the tetrazole ligand does not alter significantly the ligand field strength. Thermal spin crossover still occurs in $[Fe(mtz)_6](BF_4)_2$, but with a different behaviour, as compared to the ptz analog, as can be seen from Figures 12 and 13. Optical single-crystal absorption measurements as a function of temperature yielded the HS molar fractions as plotted in Figure 12.[76] The spin transition curve dops sharply at $T_{1/2}$ = 74 K and merges into a plateau at γ_{HS} = 0.5. The explanation for this finding comes from a single-crystal X-ray structure analysis.[77] At room temperature, the HS-iron(II) ions are accommodated in two inequivalent lattice sites A and B, with a ratio of 1:1, with slightly different lattice parameters and apparently with slightly different ligand field potentials such that only the iron ions in A-sites undergo a thermal spin transition, whereas the B-site ions remain in the HS state over the whole temperature range under study. This was nicely confirmed using Mössbauer spectroscopy (see Figure 13).

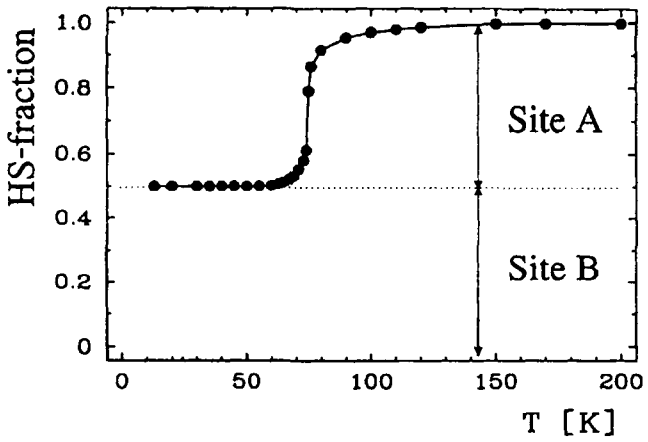

FIGURE 12 Temperature dependence of the molar fraction of HS molecules, $\gamma_{HS}(T)$, in $[Fe(mtz)_6](BF_4)_2$ determined from the area fractions of the $^1A_1 \rightarrow {}^1T_1$ absorption band of a single crystal (from ref. 76).

The Mössbauer spectra recorded between room temperature and ca. 160 K show practically only one typical HS-iron(II) quadrupole doublet.[79] Obviously, the difference between the local electric field gradients of the two kinds of lattice sites determining the size of the quadrupole splittings is too small to be resolved in the Mössbauer spectra. Below ca. 160 K, however, the two doublets HS_A and HS_B are resolved, and one observes that the HS_A doublet disappears with decreasing temperature at the favor of a new signal typical for the LS_A state.

We have carried out LIESST and reverse-LIESST experiments on $[Fe(mtz)_6](BF_4)_2$.[76,78] Figure 14 shows a selection of representative Mössbauer spectra which demonstrate the various switching processes. It starts with the spectrum obtained at 50 K after thermal spin transition. Irradiation with green light (514 nm) at 20 K con-

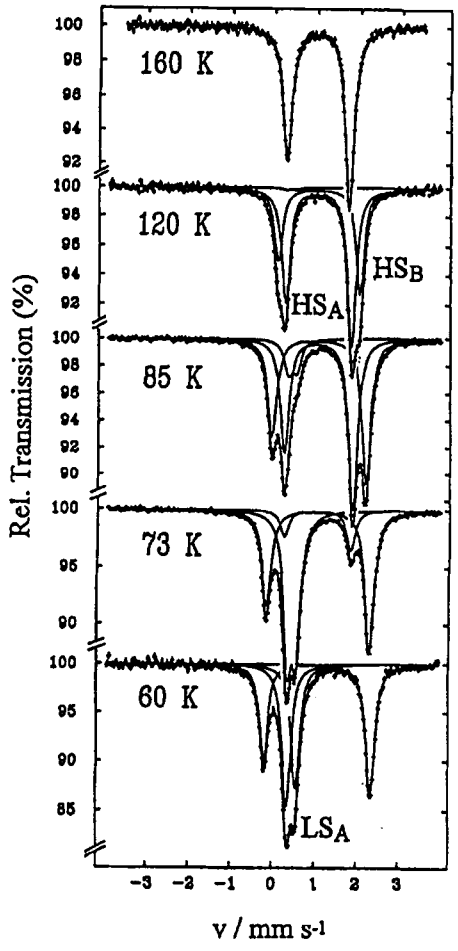

FIGURE 13 Mössbauer spectra of $[Fe(mtz)_6](BF_4)_2$ recorded at different temperatures revealing two HS doublets, HS_A and HS_B (with slightly larger quadrupole splitting for HS_B than for HS_A), due to different lattice sites A and B of iron(II) below 160 K. Only the iron ions in lattice site A undergo a thermal spin transition (from ref. 78).

verts the A-site ions quantitatively from the LS to the HS state (LIESST: $LS_A \rightarrow HS_A$). Warming the crystal up to ca. 50 K induces thermal back relaxation to the LS_A state and the spectrum of Figure 14 (a) is found to be restored. Bleaching the crystal with red light (820 nm from a Ti/sapphire laser) brings about a significant decrease of the intensity of the HS_B doublet with a simultaneous corresponding increase of the intensity of the LS signals (LIESST: $HS_B \rightarrow LS_B$) as can be seen from Figure 14 (c). This is the first example of a light-induced conversion of a stable HS iron(II) state to the metastable LS state. This was also confirmed by optical spectroscopy.[78,80] The Mössbauer subspectra arising from

LS_A and LS_B have the same parameters (isomer shift and quadrupole splitting) and cannot be resolved. The fraction of HS_A to be seen in Figure 14 (c) is due to the fact that the 820 nm irradiation hits also part of the $^1A_1 \rightarrow {}^3T_1$ absorption band thereby causing the normal LIESST effect $LS_A \rightarrow HS_A$ via $^1A_1 \rightarrow {}^3T_1 \rightarrow {}^5T_2$. Thermal relaxation experiments following the 820 nm irradiation demonstrate nicely the bistability of the metastable LS_B state: Warming up first to temperatures below 55 K leads to a complete HS→LS decay in both A and B lattice sites; cf. Figure 14 (d). The following thermal relaxation above ca. 55 K, however, causes $LS_B \rightarrow HS_B$ and simultaneously $HS_A \rightarrow LS_A$ conversion, thus again restoring the initial spectrum obtained after cooling, as can be seen from Figure 14 (e), which shows the Mössbauer spectrum taken after thermal relaxation at 64 K. The same spectrum is obtained on warming up directly to 64 K, i.e. on going from spectrum (c) to spectrum (e).

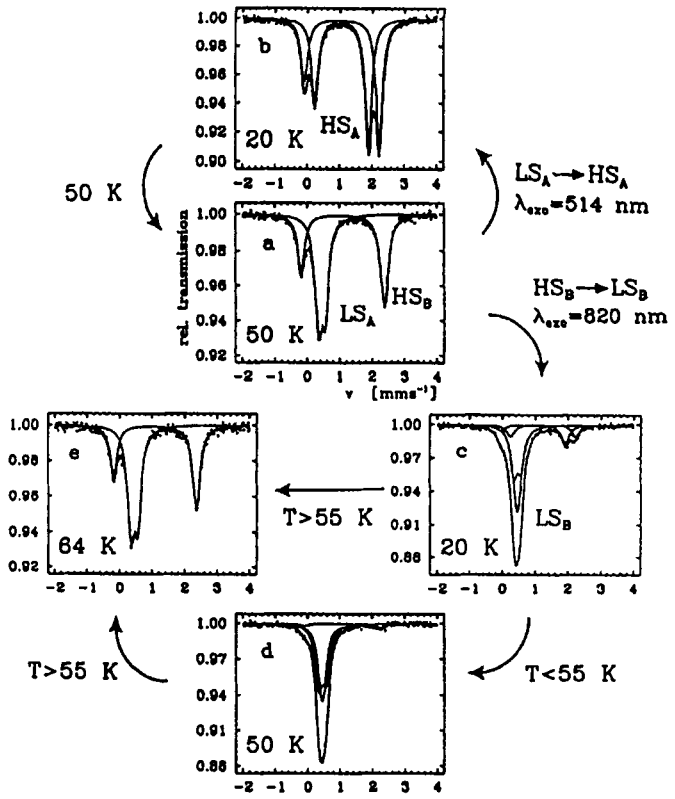

FIGURE 14 ^{57}Fe Mössbauer spectra of $[Fe(mtz)_6](BF_4)_2$ showing the thermal spin transition at site A after cooling down to 50 K (a) and the possibilities of switching the spin state at both sites with light (b,c). The metastable state in (c) exhibits a bistability as can be seen from the different thermal relaxation behaviour below and above 55 K (d,e) (adapted from ref. 76).

The relaxation processes after LIESST have, in all cases studied so far, found to be strongly influenced by cooperative effects of elastic origin, leading to characteristic deviations from first-order kinetics.[81,82] This was attributed to a buildup of an internal pres-

sure during the relaxation process, giving rise to a shift in both the horizontal (bond length difference Δr_{HL}) and the vertical (energy gap ΔE_{HL}^0) displacements of the potential wells relative to each other. This manifests itself in a self-acceleration causing the deviation from first-order decay curves. The shifts can be estimated from the observed shift of the d-d absorption bands (to be on the order of 100 cm^{-1}) as was first pointed out by Hauser.[82] Such shifts were observed on a single-crystal of $[Fe(mtz)_6](BF_4)_2$ even for both the $HS_A \rightarrow LS_A$ relaxation and the $LS_B \rightarrow HS_B$ relaxation by following the intensity of the $^1A_1 \rightarrow {}^1T_1$ absorption band in time intervals of 240 s and 360 s, respectively, at 64 K (see Figure 15).

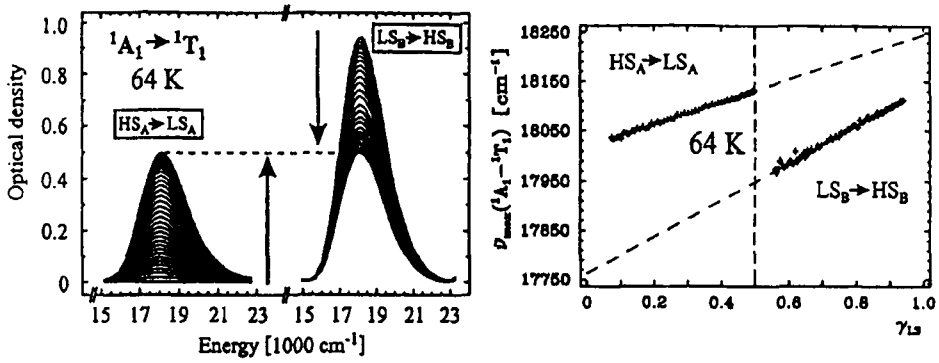

FIGURE 15 Single crystal absorption spectra of $[Fe(mtz)_6](BF_4)_2$ showing (a) the recovery of the $^1A_1 \rightarrow {}^1T_1$ absorption band at 64 K after irradiation at 514.5 nm (time interval 240 s) and (b) the decreasing intensity of the $^1A_1 \rightarrow {}^1T_1$ absorption band after irradiation at 830 nm and warming the crystal to 64 K (time interval 360 s) (adapted from ref. 80).

FIGURE 16 Shift of the $^1A_1 \rightarrow {}^1T_1$ absorption band as a function of the LS fraction γ_{LS} during (a) the $HS_A \rightarrow LS_A$ relaxation and (b) the $LS_B \rightarrow HS_B$ relaxation at 64 K (adapted from ref. 80).

Careful analysis of the position of the band maximum of the $^1A_1 \rightarrow {}^1T_1$ transition reveals a small but significant shift during the relaxation process. These shifts are displayed as a function of γ_{LS} for both relaxation processes in Figure 16.[80] It is interesting to note the different slopes for the two relaxation processes, the one for the $LS_B \rightarrow HS_B$ relaxation being steeper than that for the $HS_A \rightarrow LS_A$ relaxation. In view of our model of elastic interactions, this may well point at a softer nearby lattice surroundings with a smaller bulk modulus for the B-sites than for the A-sites, in accordance with the HS ground state (B-site) possessing lower stretching vibrational frequencies than the LS ground state (A-site).

The analogous etz complex (etz = 1-ethyl-tetrazole) behaves in a similar way, except that the A:B ratio determined by X-ray structure analysis is now 2:1.[83] Iron(II) on site A undergoes a thermal spin transition with $T_{1/2}$ = 105 K, whereas that on site B remains in the HS state down to cryogenic temperatures. Application of external pressure

of up to 1200 bar between 200 K and 60 K does not cause any formation of the LS state on site B. On site A the HS state can be populated as a metastable state at 20 K by irradiating the sample at 514.5 nm, on site B a light-induced population of the LS state can be achieved by irradiation at 820 nm.[83] The relaxation processes[84] subsequent to the HS→LS conversion on site B by LIESST reveal a light-induced bistability for the complexes on site B at 70 K. The bistability as well as the missing thermal spin transition on site B are attributed to a thermal hysteresis for the B-site complexes with a critical temperature $T_c^{\uparrow} \approx 77$ K in the heating direction. This hysteresis can be interpreted in terms of strong cooperative effects of elastic origin, which, in addition, cause characteristic deviations of the relaxation on site B from first-order kinetics (self-acceleration). In contrast, the HS→LS relaxation on site A at 60 K after irradiation with $\lambda = 514.5$ nm shows an unusual self-retardation.

LIESST in Other Iron(II) Spin Crossover Systems

The effect of light-induced spin state conversion yielding long-lived metastable states (LIESST) was observed in numerous iron(II) compounds, all of them exhibiting thermal spin transition.[7] A particularly interesting system is $[Fe(bpp)_2](BF_4)_2$ (bpp = 2,6-bis(pyrazol-3-yl)pyridine).[85,86] This compound shows a thermal spin transition with hysteresis (width ca. 10 K) near 170 K [85] and also LIESST and reverse-LIESST.[86] Mössbauer spectroscopy was employed to follow the relaxation, in the temperature range between 90 and 100 K, of the LIESST state after bleaching with green light as well as the relaxation of the metastable HS state trapped by rapidly cooling the crystals. The relaxation curves for both trapping procedures resemble each other very much. They also show strong deviations from first-order kinetics (sigmoidal decay curves) due to cooperative interactions, i.e. the relaxation processes are self-accelerating with the decay rates being a function of the LS fraction. It is worth noting that $[Fe(bpp)_2](BF_4)_2$ is the first spin crossover complex in which long-lived metastable HS states could be generated by LIESST at temperatures as high as 80 K, i.e. in the liquid nitrogen temperature region. Another interesting and unusual observation is that the saturation ratio HS/LS in the LIESST experiment at 80 K depends on the intensity of the incident laser light. This can be understood in view of a structural phase transformation; as soon as a critical fraction of HS complexes is generated by LIESST, a new structural phase will be induced which stabilizes the HS state. This new structure phase is apparently also metastable and decays within days to hours between 90 and 100 K. This secondary structural effect following LIESST may eventually lead to information storage at much higher temperatures than in case of LIESST alone, which is confined to molecular dimensions.

All the iron(II) spin crossover compounds which became known so far to show the LIESST effect have nitrogen-donating ligand molecules, with only one exception, viz. the complex $[Fe(dppen)_2Cl_2]\cdot 2CHCl_3$ (dppen = cis-1,2-bis(diphenylphosphino)ethylene). This compound contains two bidentate phosphorus-donating ligand molecules in the (x,y)-plane and two chlorine atoms in axial positions. It has been structurally characterized and also shown to exhibit thermal spin transition.[87,88] Using Mössbauer spectroscopy we carried out successfully LIESST and reverse-LIESST experiments on this compound,[89] which represents the first example for the occurrence of a light-induced spin state conversion yielding long-lived metastable states in a non-FeN_6 core complex.

NUCLEAR DECAY INDUCED EXCITED SPIN STATE TRAPPING (NIESST)

More than two decades ago we observed for the first time by Mössbauer emission

spectroscopy that the nucleogenic Fe^{2+} ions generated by the electronic capture (EC) decay of $^{57}Co^{2+}$ embedded in coordination compounds may be detected as metastable electronic states.[90] We denoted these states „anomalous spin states", because they are different from the ground spin states of the corresponding iron(II) compounds. As an example, $[Fe(phen)_3](ClO_4)_2$ is well known to be a typical strong-field coordination compound with iron(II) ions in the $^1A_1$ ground state independent of the temperature. The cobalt(II) analogue $[Co(phen)_3](ClO_4)_2$ is high spin with $^4T_1$ ground state (in the approxiamtion of O_h symmetry). If this compound is doped with ^{57}Co and used as the source in a Mössbauer emission experiment against $K_4[Fe(CN)_6]$ as a single-line absorber, one observes typical LS-iron(II) spectra near room temperature. Apparently, after the electron capture decay $^{57}Co(EC)^{57}Fe$ the oxidation state of the nucleogenic ^{57}Fe is again +2 (except for a minor fraction of Fe^{3+}). But the electronic structure adjusts rapidly (in times shorter than the time scale of ^{57}Fe Mössbauer spectroscopy, i.e. ca. 10^{-7} s) from HS-Co(II) to LS-Fe(II). At $T \leq 200$ K, however, typical HS-Fe(II) signals are seen in the Mössbauer emission spectra of this compound in addition to the LS-Fe(II) signals. The intensity of the HS-Fe(II) resonances increase with decreasing temperature at the expense of the LS-Fe(II) intensity. Obviously, the lifetime of the metastable HS-Fe(II) state is on the order of the Mössbauer time scale and becomes longer at cryogenic temperatures.

In Mössbauer emission experiments with ^{57}Co doped Co(II) compounds with weaker ligand fields corresponding to Fe(II) spin crossover compounds one only observed HS-Fe(II) resonance lines at all temperatures, even in those regions where the corresponding Fe(II) spin crossover compounds exhibit the stable $^1A_1$ ground state.[90] Examples are given in references 91-97.

The mechanism of the nuclear decay induced formation of metastable spin states of iron(II) remained largely in the dark until we discovered the LIESST phenomenon, i.e. the trapping of metastable states by irradiation with an *external* light source. The nuclear decay process $^{57}Co(EC)^{57}Fe$ may be regarded as an *internal* molecular light source, whereby energy is released due to the creation of a hole in the K-shell and due to the coulombic dilatation of the atomic volume of the nucleogenic $^{57}Fe^{2+}$ ion as compared to the parent $^{57}Co^{2+}$ ion. This energy release causes self-excitation which leads to population of excited electronic levels. In analogy to LIESST we have termed this phenomenon „Nuclear Decay-Induced Excited Spin State Trapping (NIESST)". It turns out that the mechanism of NIESST is essentially the same as for LIESST (see Figure 10), except for the initial excitation step; cf. Figure 17.

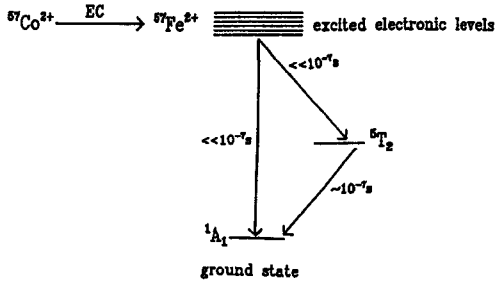

FIGURE 17 Schematic illustration of the mechanism of the nuclear decay-induced excited spin state trapping (NIESST).

There are fast (<< 10^{-7}s) spin-allowed transitions to the $^1A_1$ ground state as well as fast intersystem crossing processes (also << 10^{-7}s), which are favoured by spin-orbit coupling as in LIESST, feeding the metastable $^5T_2$ state. The lifetime of the metastable $^5T_2$ state falls into the Mössbauer time window and becomes detectable in the Mössbauer emission spectrum. The branching ratio for the two decay paths (prompt decay to the $^1A_1$ and population of the $^5T_2$ state) depends on the ligand field strength of the compound under study. The weaker the ligand field strength, the more pronounced becomes the trapping of the $^5T_2$ state. This corresponds to the observed correlation of the lifetime of the metastable LIESST state and the energy difference ΔE_{HL}^0, which also depends on the ligand field strength (*reduced energy gap law*).

The proposed mechanism for NIESST and its close resemblance to that of LIESST received strong support from the similarity of the measured lifetimes of the trapped spin states after LIESST and NIESST, respectively. We have constructed a special coincidence spectrometer for time-differential Mössbauer emission spectroscopy (TDMES) with a resolution of 3.5 ns in the time window of ca. 5 to 500 ns.[98] In case of the strong-field complex [^{57}Co/Co(phen)$_3$] we measured the lifetime of one the two metastable HS-Fe(II) states to be 390 ns (10 K), 205 ns (47 K), and 100 ns (100 K).[99] From optical spectrosopcy after laser excitation of [Fe(phen)$_3$](ClO$_4$)$_2$ embedded in a Nafion foil we determined the lifetime of the metastable $^5T_2$ state to be 188 ns at 50 K,[100] in very good agreement with the lifetime of 205 ns (47 K) after NIESST. Very recently, we studied another strong-field system, viz. a single crystal of [^{57}Co/Mn(bipy)$_3$](PF$_6$)$_2$ (bipy = 2,2'-bipyridyl) by TDMES and a single crystal of the corresponding [Fe(0.05%)//Mn(bipy)$_3$](PF$_6$)$_2$ by laser excitation and found again very good agreement between the liftetime data after NIESST and LIESST, respectively.[101]

ACKNOWLEDGEMENT

I wish to express my sincere thanks to all my colleagues and students, who have contributed to the work presented here; their names are listed in the references. Financial support from the *Deutsche Forschungsgemeinschaft, the Bundesministerium für Forschung und Technologie, the Fonds der Chemischen Industrie,* the *European Community* (Contract No. ERB CHRX CT920080), and the *Materialwissenschaftliches Forschungszentrum der Universität Mainz* is gratefully acknowledged.

REFERENCES

1. Mixed Valence Systems: Applications in Chemistry, Physics and Biology, edited by K. Prassides (Kluwer Academic Publishers, Dordrecht, 1991).
2. Mixed Valence Compounds, Theory and Applications in Chemistry , Physics, Geology and Biology, edited by D. B. Brown (D. Reidel Publishing Company, Dordrecht, Boston, London, 1979).
3. C. G. Pierpont, S. K. Larsen, S. R. Boone, Pure and Appl. Chem., 60, 1331 (1988).
4. C. G. Pierpont, R. M. Buchanan, Coord. Chem. Rev., 38, 45 (1981).
5. D. M. Adams, A. Dei, A. L. Rheingold, D. N. Hendrickson, J. Am. Chem. Soc., 115, 8221 (1993).
6. D. M. Adams, B. L. Li, J. D. Simon, D. N. Hendrickson, Angew. Chem. Int. Ed. Engl., 34, 1481 (1995).
7. P. Gütlich, H. Spiering, A. Hauser, Angew. Chem. Int. Ed. Engl., 33, 2024 (1994).
8. J. Endicott, J. Phys. Chem., 97, 3225 (1993).
9. a) Th. Woike, W. Krasser, H. Zöllner, W. Kirchner, S. Haussühl, Z. Phys., D 25, 351 (1993), b) Th. Woike, W. Kirchner, G. Schetter, Th. Barthel, K. Hyung-Sang, S. Haussühl, Optics Communications, 106, 6 (1994), c) S. Haussühl, G. Schetter, Th. Woike, Optics Communications, 114, 219 (1995).
10. M. Verdaguer, Science, 272, 698 (1996).
11. O. Sato, T. Iyoda, A. Fujishima, K. Hashimoto, Science, 272, 704 (1996).
12. O. Kahn, J. Kröber, C. Jay, Adv. Mater., 4, 718 (1992).
13. P. Gütlich, Nuclear Instruments and Methods in Physics Research, B 76, 387 (1993).
14. C. J. Ballhausen, Introduction to Ligand Field Theory (McGraw Hill Inc., New York, 1962)..
15. H. L. Schäfer, G. Gliemann, Einführung in die Ligandenfeldtheorie (Akademische Verlagsgesellschaft, Wiesbaden, 1980).
16. a) L. Cambi, A. Cagnasso, Atti Accad. Naz. Lincei, 13, 809 (1931) b) L. Cambi, L. Szegö, Ber. Dtsch. Chem. Ges., 64, 259 (1931) c) L. Cambi, L. Szegö Atti Accad. Naz. Lincei, 15, 266 (1932a) d) L. Cambi, L. Malatesta Ber. Dtsch. Chem. Ges., 70, 2067 (1937).
17. W. A. Baker, H. M. Bobonich, Inorg. Chem., 3, 1184 (1964).
18. J. Zarembowitch, New. J. Chem, 16, 255 (1992).
19. P. Gütlich, B. R. McGarvey, W. Kläui, Inorg. Chem., 19, 3704 (1980).
20. W. Kläui, W. Eberspach, P. Gütlich, Inorg. Chem., 26, 3977 (1987).
21. J. H. Ammeter, R. Bucher, N. Oswald, J. Am. Chem. Soc., 96, 7883 (1974).
22. D. M. Halepoto, D. G. L. Holt, L. F. Larkworthy, G. J. Leigh, D. C. Povey, G. W. Smith, J. Chem. Soc. Chem. Commun., 1322 (1989).
23. P. Gütlich, Struct. Bonding (Berlin), 44, 83 (1981).
24. E. König, G. Ritter, S. K. Kulshreshtha, Chem. Rev., 85, 219 (1985).
25. E. König, Prog. Inorg. Chem., 35, 527 (1987).

26. H. Toftlund, Coord. Chem. Rev., 94, 67 (1989).
27. E. König, Struct. Bonding (Berlin), 76, 51 (1991).
28. P. Gütlich, J. Jung, H. A. Goodwin in Nato ASI Series edited by E. Coronado (Kluwer Academic Publishers, Dordrecht) in press.
29. S. Decurtins, P. Gütlich, C. P. Köhler, H. Spiering, A. Hauser, Chem. Phys. Lett., 105, 1 (1984).
30. S. Decurtins, P. Gütlich, C. P. Köhler, H. Spiering, A. Hauser, Inorg. Chem., 24, 2174 (1985).
31. A. Hauser, J. Chem. Phys., 94, 2741 (1991).
32. A. Hauser, Comments Inorg. Chem., 17, 17 (1995).
33. F. Tuczek, H. Spiering, P. Gütlich, Hyperfine Interact., 62, 109 (1990).
34. P. Gütlich, J. Ensling, F. Tuczek, Hyperfine Interact., 84, 447 (1994).
35. M. Sorai, S. Seki, J. Phys. Chem. Solids, 35, 555 (1974).
36. H. Spiering, E. Meissner, H. Köppen, E. W. Müller, P. Gütlich, Chem. Phys., 68, 65 (1982).
37. N. Willenbacher, H. Spiering, J. Phys. C: Solid State Phys., 21, 1423 (1988).
38. H. Spiering, N. Willenbacher, J. Phys.: Condens. Matter., 1, 10089 (1989).
39. C. P. Köhler, R. Jakobi, E. Meissner, L. Wiehl, H. Spiering, P. Gütlich, J. Phys. Chem. Solids, 51, 239 (1990).
40. M. Mikami, M. Konno, Y. Saito, Chem. Phys. Lett., 63, 566 (1979).
41. J. D. Eshelby, in Solid State Phys., (Academic Press, New York, 1956), vol. 3, p. 79.
42 G. Leibfried, N. Breuer, in Springer Tracts in Modern Physics, (Springer Verlag, Berlin, 1978), vol. 81, p. 147.
43. L. Wiehl, G. Kiel, C. P. Köhler, H. Spiering, P. Gütlich, Inorg. Chem., 25, 1565 (1986).
44. L. Wiehl, H. Spiering, P. Gütlich, K. Knorr, J. Appl. Crystallogr., 23, 151 (1990).
45. C. P. Slichter, H. G. Drickamer, J. Chem. Phys., 56, 2142 (1972).
46. M. Sorai, J. Ensling, K. M. Hasselbach, P. Gütlich, Chem. Phys., 20, 197 (1977).
47. I. Sanner, E. Meissner, H. Köppen, H. Spiering, P. Gütlich, Chem. Phys., 68, 65 (1982).
48. P. Adler, L. Wiehl, E. Meissner, C. P. Köhler, H. Spiering, P. Gütlich, J. Phys. Chem. Solids, 48, 517 (1987).
49. J. Jung, F. Bruchhäuser, R. Feile, H. Spiering, P. Gütlich, Z. Phys., B 100, 523 (1996).
50. J. Jung, Ph. D. thesis, Johannes Gutenberg-Universität Mainz, 1995.
51. H. Köppen, E. W. Müller, C. P. Köhler, H. Spiering, E. Meissner, P. Gütlich, Chem. Phys. Lett., 91, 348 (1982).
52. V. Petrouleas, J. P. Tuchagues, Chem. Phys. Lett., 137, 21 (1987).
53. J.-A. Real, H. Bolvin, A. Bousseksou, A. Dworkin, O. Kahn, F. Varret, J. Zarembowitch, J. Am. Chem. Soc., 114, 4650 (1992).
54. M. Kaji, M. Sorai, Thermochim. Acta, 88, 185 (1985).
55. R. Jakobi, H. Spiering, P. Gütlich, J. Phys. Chem. Solids, 53, 267 (1992).

56. T. Kohlhaas, H. Spiering, P. Gütlich, submitted to Z. Phys. B.
57. E. König, G. Ritter, J. Waigel, H. A. Goodwin, J. Chem. Phys., 83, 3055 (1985).
58. T. Garnier, B. Gallois, J. Gaultier, J.-A. Real, J. Zarembowitch, Inorg. Chem., 32, 5305 (1993).
59. G. J. Long, B. B. Hutchinson, Inorg. Chem., 26, 608 (1987).
60. J. K. McCusker, M. Zvagulis, H. H. Drickamer, D. N. Hendrickson, Inorg. Chem., 28, 1380 (1989).
61. T. Kambara, N. Sasaki, J. Phys. Soc. Jpn., 51, 1694 (1982).
62. N. Sasaki, T. Kambara, J. Phys. Soc. Jpn., 56, 3956 (1987).
63. N. Sasaki, T. Kambara, Phys. Rev. B 40, 2442 (1989).
64. A. Bousseksou, J. Nasser, J. Linares, K. Boukheddaden, F. Varret, J. Phys. I France, 2, 1381 (1992).
65. K. Takahashi, Z. Phys. B Condensed Matter, 71, 205 (1988).
66. H. Bolvin, O. Kahn, Chem. Phys., 192, 295 (1995).
67. J. Linares, J. Nasser, K. Boukheddaden, A. Bousseksou, F. Varret, J. Magn. Magn. Mater., 140, 1507 (1995).
68. J. Linares, J. Nasser, A. Bousseksou, K. Boukheddaden, F. Varret, J. Magn. Magn. Mater., 140, 1503 (1995).
69. J. Jung, F. Bruchhäuser, R. Feile, H. Spiering, P. Gütlich, Z. Phys. B 100, 517 (1996).
70. A. Hauser, Chem. Phys. Lett., 124, 543 (1986).
71. R. Jakobi, H. Romstedt, H. Spiering, P. Gütlich, Angew. Chem. Int. Ed. Engl., 31, 178 (1992).
72. H. Romstedt, H. Spiering, P. Gütlich, unpublished results.
73. E. Bukhs, G. Navon, M. Bixon, J. Jortner, J. Am. Chem. Soc., 102, 2918 (1980).
74. P. Adler, H. Spiering, P. Gütlich, Inorg. Chem., 26, 3840 (1980).
75. P. Adler, H. Spiering, P. Gütlich, J. Phys. Chem. Solids, 50, 587 (1989).
76. R. Hinek, Ph. D. thesis, Johannes Gutenberg-Universität Mainz, 1995.
77. L. Wiehl, Acta Cryst. B, 49, 289 (1993).
78. P. Poganiuch, S. Decurtins, P. Gütlich, J. Am. Chem. Soc., 112, 3270 (1990).
79. P. Gütlich, R. Link, A. X. Trautwein, Mössbauer Spectroscopy and Transition Metal Chemistry (Springer Verlag, Berlin, 1978).
80. R. Hinek, A. Hauser, P. Gütlich, Inorg. Chem., 33, 567 (1994).
81. A. Hauser, P. Gütlich, H. Spiering, Inorg. Chem., 25, 4245 (1986).
82. A. Hauser, Chem. Phys. Lett., 192, 65 (1992).
83. R. Hinek, H. Spiering, D. Schollmeyer, P. Gütlich, A. Hauser, Chem. Eur. J., in press (to appear in Nov. 1996).
84. R. Hinek, H. Spiering, P. Gütlich, A. Hauser, Chem. Eur. J., in press (to appear in Nov. 1996).
85. K. H. Sugiyarto, H. A. Goodwin, Aust. J. Chem., 41, 1645 (1988).
86. Th. Buchen, P. Gütlich, H. A. Goodwin, Inorg. Chem., 33, 4573 (1994).
87. F. Cecconi, M. Di Vara, S. Midollini, A. Orlandini, L. Sacconi, Inorg. Chem., 20, 3423 (1981).

88. E. König, G. Ritter, S. K. Kulshreshtha, J. Waigel, L. Sacconi, Inorg. Chem., 23, 1241 (1984).
89. C.-C. Wu, J. Jung, K. M. Sena, D. N. Hendrickson, P. Gütlich, to be published.
90. H. Sano and P. Gütlich, Hot Atom Chemistry in Relation to Mössbauer Emission Spectroscopy in Hot Atom Chemistry, edited by T. Matsuura (Tokyo, 1984).
91. J. Ensling, P. Gütlich, K. M. Hasselbach, B. W. Fitzsimmons, Chem. Phys. Lett., 42, 232 (1976).
92. J. Ensling, B. W. Fitzsimmons, P. Gütlich, K. M. Hasselbach, Angew. Chem., 9, 637 (1970).
93. J. Fleisch, P. Gütlich, Chem. Phys. Lett., 42, 237 (1976).
94. J. Fleisch, P. Gütlich, Chem. Phys. Lett., 45, 29 (1977).
95. J. Fleisch, P. Gütlich, H. Köppen, Radiochem. Radioanalyt. Lett., 42, 279 (1980).
96. P. Gütlich, H. Köppen, J. Physique, Colloque C1, suppl. No.1, 41, C1 (1980).
97. C. Hennen, Master's thesis, D77, Johannes Gutenberg-Universität Mainz 1986.
98. R. Albrecht, M. Alflen, P. Gütlich, Zs. Kajcsos, R. Schulze, H. Spiering, F. Tuczek, Nucl. Instr. Meth., A257, 209 (1987).
99. R. Grimm, P. Gütlich, E. Kankeleit, R. Link, J. Chem. Phys., 67, 5491 (1977).
100. A. Hauser, Chem. Phys. Lett., 173, 507 (1990).
101. S. Deisenroth, A. Hauser, H. Spiering, P. Gütlich, Hyperfine Interact., 93, 1573 (1994).